

220 μ J monolithic single-frequency Q-switched fiber laser at 2 μ m by using highly Tm-doped germanate fibers

Wei Shi,^{1,*} Eliot B. Petersen,^{1,2} Dan T. Nguyen,¹ Zhidong Yao,¹ Arturo Chavez-Pirson,¹ N. Peyghambarian,^{1,3} and Jirong Yu⁴

¹NP Photonics Inc., 9030 S Rita Rd, Tucson, Arizona 85747, USA

²Physics Department, University of Arizona, Tucson, Arizona 85721, USA

³College of Optical Sciences, University of Arizona, Tucson, Arizona 85721, USA

⁴NASA Langley Research Center, 5 North Dryden Street, Hampton, Virginia 23681, USA

*Corresponding author: wshi@npphotonics.com

Received July 8, 2011; revised August 13, 2011; accepted August 13, 2011;

posted August 15, 2011 (Doc. ID 150765); published September 9, 2011

We report a unique all fiber-based single-frequency Q-switched laser in a monolithic master oscillator power amplifier configuration at \sim 1920 nm by using highly Tm-doped germanate fibers for the first time. The actively Q-switched fiber laser seed was achieved by using a piezo to press the fiber in the fiber Bragg grating cavity and modulate the fiber birefringence, enabling Q-switching with pulse width and repetition rate tunability. A single-mode polarization maintaining large core 25 μ m highly Tm-doped germanate fiber was used in the power amplifier stage. For 80 ns pulses with 20 kHz repetition rate, we achieved 220 μ J pulse energy, which corresponds to a peak power of 2.75 kW with transform-limited linewidth. © 2011 Optical Society of America

OCIS codes: 140.3540, 060.3735, 140.3510, 060.2320.

Currently, fiber-based Q-switched lasers have attracted intense interest due to their unique advantages of compactness, high peak power, robustness, and low maintenance. Q-switched fiber lasers have many potential applications in such areas as fiber based LIDAR, remote sensing, and nonlinear frequency generation. Several approaches have been reported to achieve Q-switched fiber lasers. For example, free-space or fiber pigtailed acousto-optical modulator and electro-optical modulator are used in the fiber laser cavity [1]. Saturable absorbers are used to achieve the passive Q-switched fiber lasers [2]. All-fiber Q-switched lasers using nonlinearities such as Raman backscattering have been constructed [3]. Other actively Q-switching all-fiber lasers include magnetostriction modulation of fiber Bragg gratings (FBGs), stretching of FBGs with piezoelectric elements, acoustically generated microbending, and evanescent field coupling [4,5].

In order to achieve transform-limited nanosecond fiber laser pulses, all-fiber single-frequency actively Q-switched lasers at \sim 1 μ m and \sim 1.5 μ m were reported based on induced birefringence and highly doped phosphate fibers in the cavity [6–8]. These Q-switched fiber laser pulses have been successfully used in nonlinear frequency conversion and laser remote sensing [9,10]. In this method, a piezoelectric compresses a fiber creating stress birefringence, and this birefringence acts as a waveplate, changing the polarization state of the light in the fiber. This Q-switch mechanism is similar to using an electro-optic modulator, where the polarization is modulated to switch the laser between high and low feedback states. Most recently, a single-frequency 1.95 μ m Q-switched fiber laser was reported by using induced birefringence and Tm-doped silicate fiber in the cavity [11]. There have been important reports of high peak-power amplifiers and high pulse energy Q-switched lasers operating at 1.9 μ m based on Tm-doped fluoride and silica

fibers, respectively [12,13]; however, in these previous reports the pulses are spectrally broad, and thus less sensitive to SBS effects compared to spectrally narrow, transform-limited pulses. In this Letter, we report an all-fiber single-frequency actively Q-switched laser operating at \sim 1920 nm by using a piezo to press the fiber in the FBG cavity based on highly Tm-doped germanate fiber, for the first time. Moreover, a monolithic master oscillator power amplifier (MOPA) based fiber laser system has been implemented based on a new single-mode (SM) polarization maintaining (PM) large core 25 μ m highly Tm-doped germanate fiber. For the transform-limited 80 ns pulses with repetition rate of 20 kHz, we achieved 220 μ J pulse energy, which is the highest value for longer ns transform-limited pulses in 2 μ m regime, and corresponds to a peak power of 2.75 kW.

Figure 1 shows the schematic of the implemented single-frequency Q-switched fiber laser at \sim 1920 nm in MOPA configuration. For the Q-switched fiber laser seed, the cavity consists of our proprietary highly Tm-doped (5% wt) germanate glass fiber (TGF) with core size \sim 7 μ m. The high doping concentration creates a high unit gain in active fiber, allowing for a 2 cm cavity length that is significantly shorter than other Q-switched fiber lasers.

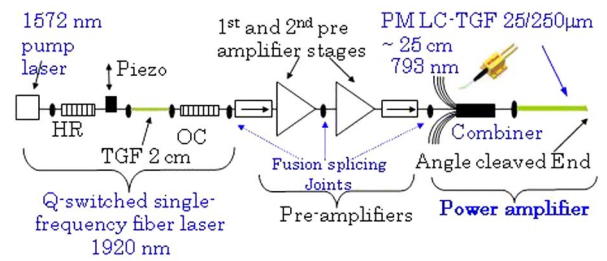


Fig. 1. (Color online) Schematic of monolithic single-frequency Q-switched fiber laser at 1920 nm in MOPA configuration. HR, high reflectivity grating; OC, output coupler grating; TGF, highly Tm-doped germanate fiber.

Report Documentation Page			<i>Form Approved OMB No. 0704-0188</i>	
<p>Public reporting burden for the collection of information is estimated to average 1 hour per response, including the time for reviewing instructions, searching existing data sources, gathering and maintaining the data needed, and completing and reviewing the collection of information. Send comments regarding this burden estimate or any other aspect of this collection of information, including suggestions for reducing this burden, to Washington Headquarters Services, Directorate for Information Operations and Reports, 1215 Jefferson Davis Highway, Suite 1204, Arlington VA 22202-4302. Respondents should be aware that notwithstanding any other provision of law, no person shall be subject to a penalty for failing to comply with a collection of information if it does not display a currently valid OMB control number.</p>				
1. REPORT DATE 09 SEP 2011	2. REPORT TYPE	3. DATES COVERED 00-00-2011 to 00-00-2011		
4. TITLE AND SUBTITLE 220 &#956;J monolithic single-frequency Q-switched fiber laser at 2 &#956;m by using highly Tm-doped germanate fibers			5a. CONTRACT NUMBER	
			5b. GRANT NUMBER	
			5c. PROGRAM ELEMENT NUMBER	
6. AUTHOR(S)			5d. PROJECT NUMBER	
			5e. TASK NUMBER	
			5f. WORK UNIT NUMBER	
7. PERFORMING ORGANIZATION NAME(S) AND ADDRESS(ES) NP Photonics, Inc,UA Science & Technology Park,9030 S. Rita Rd. - Suite 120,Tucson,AZ,85747			8. PERFORMING ORGANIZATION REPORT NUMBER	
9. SPONSORING/MONITORING AGENCY NAME(S) AND ADDRESS(ES)			10. SPONSOR/MONITOR'S ACRONYM(S)	
			11. SPONSOR/MONITOR'S REPORT NUMBER(S)	
12. DISTRIBUTION/AVAILABILITY STATEMENT Approved for public release; distribution unlimited				
13. SUPPLEMENTARY NOTES				
14. ABSTRACT				
15. SUBJECT TERMS				
16. SECURITY CLASSIFICATION OF:			17. LIMITATION OF ABSTRACT Same as Report (SAR)	18. NUMBER OF PAGES 3
a. REPORT unclassified	b. ABSTRACT unclassified	c. THIS PAGE unclassified	19a. NAME OF RESPONSIBLE PERSON	

This short cavity length creates large longitudinal mode spacing, helping to maintain lasing on a single longitudinal mode. The active fiber is fusion-spliced between two FBGs as shown in Fig. 1. One FBG has a high reflectivity (HR) grating imprinted on a non-PM silica fiber. The other FBG, the output coupler (OC), has a low reflectivity grating made on a PM fiber, creating a different reflection wavelength for each polarization, with each grating having ~ 5 GHz of bandwidth. The reflection band of the high reflector is matched to only one of the reflection bands of the OC, making the laser cavity polarization dependent. Between the HR-FBG and active fiber, a few millimeters silica fiber was stressed by a piezo to producing birefringence. The orientation of the stress was keyed at an angle of 45 degrees with respect to the slow and fast axis of the PM fiber in order to obtain a high modulation contrast. A SM fiber laser at 1572 nm pumps the cavity. The pump threshold at 1572 nm for this single-frequency fiber laser is about 120 mW.

Figure 2 shows the measured tunability of pulse width by simply adjusting the pump level and repetition rate. One can see that the pulse duration increases when repetition rate increases, and decreases when the pump power increases. The pulse width can be tuned from tens of ns to 300 ns by changing the pump power or repetition rate. The repetition rate can be tuned from 100 Hz to hundreds of kHz. Figure 3 shows the typical pulse shape and spectrum of the Q-switched fiber laser pulses. The pulse shapes were recorded by using a fast $\sim 2 \mu\text{m}$ detector and a fast oscilloscope, and the spectrum was measured using a modified optical spectrum analyzer. One can see that the Q-switched pulses exhibit nearly Gaussian shape.

The single-frequency performance of this Q-switched fiber laser has been verified by using a fiber-based Fabry-Perot with a free spectral range of ~ 0.91 GHz and Finesse of ~ 157 [6,8]. Insert of Fig. 3's spectrum shows the scanning spectrum for 200 ns Q-switched fiber laser pulses. One can see that the scanning Fabry-Perot spectrum shows the single burst under transmission peaks of the Fabry-Perot, which corresponds to the linewidth of <5.8 MHz that is the bandwidth limit of the Fabry-Perot interferometer [6,8].

Figure 4 shows the power output and pulse energy after the isolator for the Q-switched fiber laser seed at different repetition rates when the pump power is ~ 300 mW. From Fig. 4(a), one can see when the repetition rate increases from 1 kHz to 300 kHz, the average power is from 0.048 mW to ~ 9 mW (saturated). From

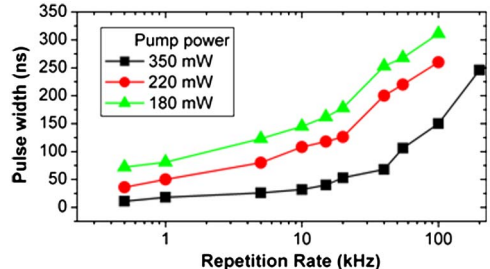


Fig. 2. (Color online) Measured pulse width tunability of Q-switched fiber laser at different pump power and repetition rates.

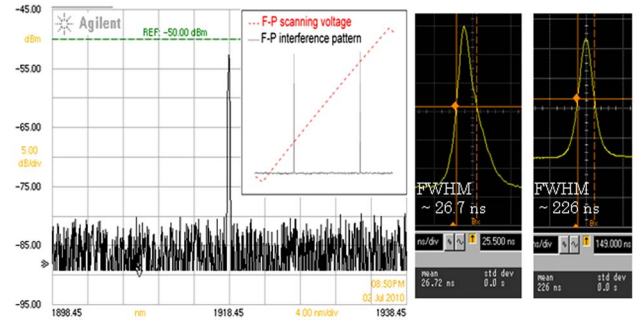


Fig. 3. (Color online) Spectrum and typical pulse shapes of single-frequency Q-switched fiber laser seed.

Fig. 4(b), in the repetition range of 1 kHz–300 kHz, the peak power is from ~ 3 W to ~ 0.1 W, and the pulse energy has the highest value of 75.5 nJ at 20 kHz.

In order to scale the pulse energy or peak/average for the Q-switched fiber laser seed, all fiber-based cascade amplifiers were implemented as shown in Fig. 1. Our MOPA-based pulsed fiber laser system is based on all-fiber monolithic components. We used commercially available isolators, pump combiners, and WDMs. For the longer ns transform-limited pulses, the main limit for the energy or power scaling is the stimulated Brillouin scattering (SBS) in the fiber amplifiers [6–10]. Therefore, we used the newly developed larger core SM PM highly Tm-doped (4%) germanate fiber LC-TGF 25/250 in the power amplifier stage shown in Fig. 1. This new germanate fiber LC-TGF 25/250 has core NA = 0.054 with core/cladding sizes 25/250 μm . Firstly, the Q-switched $\sim 2 \mu\text{m}$ fiber laser pulses with duration of ~ 80 ns at 300 mw pump power and repetition rate 20 kHz were scaled by two preamplifiers using the commercial SM PM Tm-doped silica fiber shown in Fig. 1. After the Q-switched fiber laser and between the two amplifiers, two isolators were spliced in the MOPA chain in order to block the backward amplified spontaneous emission (ASE) and any back reflections of signal. Between the two preamplifier stages, we used a narrow band filter to further suppress the ASE component. We measured the pulse energy by using a fast Ophir PE9F-SH pyroelectric energy meter. This pulse

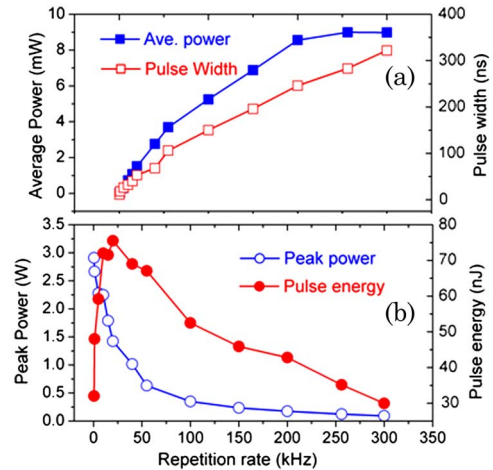


Fig. 4. (Color online) (a) Average power and pulse width, and (b) peak power and pulse energy at different repetition rates when the pump power is ~ 300 mW for the Q-switched fiber laser seed.

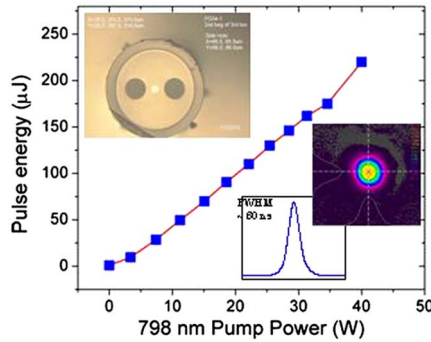


Fig. 5. (Color online) Output pulse energy for the power amplifier stage at different pump level. Insets: cross section of the new germanate fiber 25/250, beam profile image, and the pulse shape.

energy meter is insensitive to the ASE background and CW signal component. After the first preamplifier stage, the SBS-free pulse energy can be up to $1.2\text{ }\mu\text{J}$, and the pulse width is the same as the pulse width of the Q-switched seed. In the second preamplifier stage, we use a cladding pump configuration. Two multimode diodes at 798 nm (single emitters) are used to pump commercial double cladding Tm-doped fiber PM-TDF-10/130 ($\sim 2\text{ m}$) through a $(2 + 1) \times 1$ signal pump combiner. The SBS-free pulse energy can be scaled up to $\sim 14\text{ }\mu\text{J}$ after the second preamplifier stage. The power gain is about 10 dB for the second preamplifier stage. The signal to noise ratio can be close to 30 dB from the spectrum. We did not observe pulse width or shape distortion for the amplified pulses after the second amplifier stage when the pulse energy $< 14\text{ }\mu\text{J}$.

In the power amplifier stage, the new developed SM PM highly Tm-doped germanate fiber LC-TGF 25/250 was used. Inset of Fig. 5 shows the cross section of the new germanate fiber. The length of LC-TGF active fiber in the power amplifier is only $\sim 25\text{ cm}$. The output end of the LC-TGF was angle cleaved to minimize the end feedback. A commercial SM PM $(6 + 1) \times 1$ signal pump combiner was used to combine commercial fiber pigtailed single emitters at 798 nm. The 25 cm LC-TGF was fusion spliced with the output fiber of the commercial combiner based on an asymmetric fusion splicing technique. The combiner output silica fiber has the same core/cladding sizes ($25/250\text{ }\mu\text{m}$) with the new developed highly Tm-doped germanate fiber LC-TGF 25/250.

Figure 5 shows the pulse energy output for the power amplifier stage at different pump levels. One can see that the maximum pulse energy can be up to $220\text{ }\mu\text{J}$, free of SBS. For the 1920 nm pulse seed we used, the repetition rate is 20 kHz and the pulse duration $\sim 80\text{ ns}$. After the power amplifier stage, the Gaussian-like pulse shape has no obvious change, shown as an inset in Fig. 5, and the pulse duration is still about 80 ns. From the measured output pulse energy in Fig. 5, we can calculate the maximum peak power as 2.75 kW, corresponding to an average power of 4.4 W. This peak power is the highest value for transform-limited longer ns pulses in $2\text{ }\mu\text{m}$ regime.

For the power amplifier stage, the power conversion efficiency is about 12.7%, which can be improved by optimizing the seed pulse conditions as well as the fiber length of LC-TGF 25/250 in the power amplifier stage. For the amplified fiber laser 80 ns pulses ($> 200\text{ }\mu\text{J}$), the measured spectrum is very similar with the spectrum in Fig. 3, and the signal to noise ratio is close to 30 dB from the spectrum. The measured polarization extinction ratio is ~ 18 dB. The linewidth is transform-limited from the Fabry-Perot scanning spectrum, and the output beam is close to diffraction limited from the beam profile image (insets in Fig. 5).

In conclusion, we have successfully implemented a unique all fiber-based single-frequency Q-switched laser in MOPA configuration at $\sim 1920\text{ nm}$ by using highly Tm-doped germanate fibers, for the first time. The compact actively Q-switched fiber laser seed was achieved by using a piezo in the short fiber laser cavity. In the monolithic MOPA-based pulsed fiber laser system, a new developed SM PM large core highly Tm-doped germanate fiber 25/250 was used in the power amplifier stage. For the longer ns fiber laser pulses ($\sim 80\text{ ns}$), we have achieved the highest pulse energy of $220\text{ }\mu\text{J}$, which corresponds to a peak power of 2.75 kW with transform-limited linewidth.

This work has been supported by NASA Small Business Innovation Research (SBIR) project NX11CG95P, and Air Force Research Laboratory/Materials and Manufacturing Directorate SBIR project FA8650-10 C-5208. The authors acknowledge the technical support from Dr. Adam Cooney.

References

1. A. Alvarez-Chavez, H. L. Offerhaus, J. Nilsson, P. W. Turner, W. A. Clarkson, and D. J. Richardson, *Opt. Lett.* **25**, 37 (2000).
2. R. Paschotta, R. Häring, E. Gini, H. Melchior, U. Keller, H. L. Offerhaus, and D. J. Richardson, *Opt. Lett.* **24**, 388 (1999).
3. Y. Zhao and S. D. Jackson, *Opt. Lett.* **31**, 751 (2006).
4. N. Russo, R. Duchowicz, J. Mora, J. Cruz, and M. Andres, *Opt. Commun.* **210**, 361 (2002).
5. P. Pérez-Millán, J. L. Cruz, and M. V. Andrés, *Appl. Phys. Lett.* **87**, 011104 (2005).
6. W. Shi, E. Petersen, M. Leigh, J. Zong, Z. Yao, A. Chavez-Pirson, and N. Peyghambarian, *Opt. Express* **17**, 8237 (2009).
7. W. Shi, M. Leigh, J. Zong, and S. Jiang, *Opt. Lett.* **32**, 949 (2007).
8. M. Leigh, W. Shi, J. Zong, S. Jiang, and N. Peyghambarian, *Opt. Lett.* **32**, 897 (2007).
9. W. Shi, M. Leigh, J. Zong, Z. Yao, D. Nguyen, A. Chavez-Pirson, and N. Peyghambarian, *IEEE J. Sel. Top. Quantum Electron.* **15**, 377 (2009).
10. W. Shi, E. Petersen, D. T. Nguyen, Z. Yao, J. Zong, M. A. Stephen, A. Chavez-Pirson, and N. Peyghambarian, *Opt. Lett.* **35**, 2418 (2010).
11. J. Geng, Q. Wang, T. Luo, F. Amzajerdian, and S. Jiang, *Opt. Lett.* **34**, 3713 (2009).
12. M. Eichhorn, *Opt. Lett.* **30**, 3329 (2005).
13. M. Eichhorn and S. D. Jackson, *Opt. Lett.* **32**, 2780 (2007).